STUDIA UBB CHEMIA, LXIX, 2, 2024 (p. 121-134)
(RECOMMENDED CITATION)
DOI:10.24193/subbchem.2024.2.09

WEAK INTERACTIONS BETWEEN HYDRACIDS / BINARY ACIDS: SOME CONSIDERATIONS FROM A DFT ANALYSIS

Luana RADU[a], Alexandru LUPAN[a], Maria LEHENE[a], Radu SILAGHI-DUMITRESCU[a]*

ABSTRACT. Non-covalent interactions involving element-hydrogen contacts are a central part in supramolecular chemistry and play essential roles in biomolecular structure. Reported here is a systematic computational analysis of such interactions within XH_n---YH_m dimers, where X and Y are C, Si, N, P, O, S, F and Cl, respectively. Two functionals are employed – the widely used BP86 and the M06-2X functional especially designed for describing noncovalent interactions. The interaction energies are found to be correlated with charge separation to a degree of 80%, suggesting that these noncovalent interactions can be reasonably explained/predicted by their electrostatic component. Energy decomposition analyses on the other hand suggest that correlation effects are the underlying root of the interaction. The rarely discussed intermolecular vibrations are also analyzed and noted to sometimes intercede in the typical observation windows for molecular spectroscopy. Moreover, in some cases notable effects of the non-covalent interactions are noted upon internal vibrations of the partners.

Keywords: *hydracid, binary acid, noncovalent, DFT, supramolecular*

INTRODUCTION

Non-covalent interactions involving element-hydrogen contacts are a central part in supramolecular chemistry and play essential roles in biomolecular structure. Their accurate computational description has been

[a] *Faculty of Chemistry and Chemical Engineering, Babeș-Bolyai University, Str. Arany Janos Nr. 11, RO-400028 Cluj-Napoca, Romania*
* *Correspondence to: radu.silaghi@ubbcluj.ro*

described extensively, with the importance of very high-level / accurate methods often highlighted.[1–4] We have, on the other hand, shown elsewhere that accurate description of larger, real-life systems whose geometry is based dominantly on hydrogen bonds or on other non-covalent interactions is still elusive despite overconfident statements to the contrary.[5–14]

Chemical Reviews was among the first review journals to recognize the significance of non-covalent interactions and published the first thematic issue on the subject in 1988. Similar reviews followed in 1994, 2000 and 2016.[15]

A series of dimers analyzed in this paper have been also studied in literature, such as: H_2O•••NH_3, HF•••CH_4, H_2O•••CH_4, HF•••HCl, H_2O•••H_2O, H_2O•••HF, HCl•••H_2O, etc. The dimers of H_2O and HF are among the most studied systems for hydrogen bonding. The investigation of the H_2O•••HF dimer dates back to 1969 when Kollman and Allen performed the first semiempirical and later ab initio studies of this dimer. The existence of this dimer was confirmed by microwave spectroscopy in 1975. The energies and frequencies of the H_2O•••HF dimer have been calculated with CCSD(T) and MP2 methods, and the results from this level of theory provide dissociation energies and frequencies appropriate to experimental values.[16]

The heterogenous dimer, HF•••HCl was first characterized in 1977, but the only configuration detected was ClH•••FH in the microwave spectra of the molecular beam electric resonance experiments. Several years later, Fraser and Pine observed the FH•••ClH configuration in the microwave and infrared (IR) spectra of molecular beams created by expanding a mixture of HCl and HF in helium. Following the characterization (through full geometry optimizations and vibrational frequency analyses) of this system it was concluded that there is an electronic preference of HF to donate and of HCl to accept a hydrogen bond in this dimer.[16]

Reported here is a systematic computational analysis of the non-covalent interactions within H_nX---H_nY dimers, where n=1-4 and X and Y are C, Si, N, P, O, S, F and Cl, respectively. Two functionals are employed – the widely used BP86 and the M06-2X functional especially designed for describing noncovalent interactions.[2]

RESULTS AND DISCUSSION

DFT calculations were performed with two functionals, M06-2X and BP86, to explore the order of magnitude of the dependence of the results on methodology. The M06-2X functional was designed specifically for the study of non-covalent interactions, and thus parametrized to take into account long-

range dispersions. To this extent, at least in its initial report, corrections now common for other functionals (such as Grimme's dispersion) were deemed superfluous for M06-2X.[1,2,17,18] Its performance on describing structures that rely primarily on supramolecular interactions has previously been shown to be distinctly better than that of other methods.[11,12] The BP86 functional was chosen as an example of functional in general use, with the observation that the M06-2X functional in known to far outperforms BP86 and other classical functionals in describing weak interactions; however, in most cases of practical interest classical functionals are still the choice – as M06-2X fails dramatically in, e.g., describing spin states and geometries at transition metal systems.[8–13,19–27] In this context, the BP86 data may be taken as illustrating the degree to which DFT functionals can deviate from the optimum results – while the M06-2X data would be (one of) the optimal functional(s) to employ for the task (of examining systems whose geometry relies entirely on non-covalent interactions). Tables 1 and 2 show the key geometrical parameter in the dimers examined here – i.e. the intermolecular H---X contact, alongside the binding energy between the two monomers. In order to evaluate the computed H---X distance (D), the Tables also shows the sums of van der Waals radii for the respective H---X pair; an attractive interaction should entail a value of D lower than this sum. To offer a measure of the significance of the difference between the DFT-calculated distance D, and the sum of van der Waals radii, also listed in the Tables is a value R defined as the average between the sum of the van der Waals radii and the sum of the covalent radii of the respective atoms. In the ensuing discussion, unless otherwise specified, the M06-2X data are interpreted.

With few exceptions, the distances between atoms that are involved in non-covalent interactions increase as a larger molecule is involved in the system and if the number of hydrogen atoms in the molecule increases. The average distances (obtained by calculating the arithmetic mean of all interactions of the same type from different systems) for each type of interaction are: H---Cl 3.10 Å, H---F 2.39 Å, H---O 2.16 Å, H---S 2.77 Å, H---N 2.25 Å, H---P 3.05 Å, H---C 2.87 Å, H---Si 3.30 Å. The smallest distances (D) identified for each type of interaction are: H---Cl 2.45 Å, H---F 1.82 Å, H---O 1.75 Å, H---S 2.4 Å, H---N 1.67 Å, H---P 2.49 Å, H---C 2.38 Å, H---Si 2.58 Å. The largest distances identified for each type of interaction are: H---Cl 3.33 Å, H---F 2.91 Å, H---O 3.29 Å, H---S 3.04 Å, H---N 3.04 Å, H---P 3.64 Å, H---C 3.33 Å, H---Si 3.66 Å.

Thus, it is observed that the stronger interactions generally settle at values around 2.5 Å; however, there are non-covalent interactions even at distances of about 1.75 Å, while the weaker interactions settle at 3.04 Å, 3.33 Å, 3.66 Å, i.e. at distances greater than 3 Å. Compared to R (R representing the

average between the sum of the van der Waals radii and the sum of the covalent radii of the atoms involved in a non-covalent interaction), the closest and most distant interactions are established at the following distances for each type of interaction: H- --Cl 0.3 Å, respectively 1.18 Å, H---F 0.05 Å, respectively 1.04 Å, H---O 0.04 Å, respectively 1.38 Å, H--- S 0.21 Å and 1.02 Å respectively, H---N 0.05 Å and 1.11 Å respectively, H---P 0.28 Å and 1.43 Å respectively, H---C 0.38 Å and 1.33 Å, H---Si 0.47 Å and 1.08 Å, respectively. Compared to the calculated average distances, the closest and the farthest interactions are set at the following distances for each type of interaction: H---Cl 0.23 Å and 0.65 Å, respectively, H---F 0.51 Å, respectively 0.57 Å, H---O 0.41 Å, respectively 1.12 Å, H---S 0.37 Å, respectively 0.43 Å, H---N 0.57 Å, respectively 0.79 Å, H---P 0.55 Å respectively 0.59 Å, H---C 0.46 Å respectively 0.49 Å, H---Si 0.25 Å respectively 0 .35 Å. Marked in Tables 1 and 2 in italics are the instances where the predicted intermolecular contacts are larger than the sums of van der Waals radii: ClH---ClH, OH_2--- SiH_4, SH_2---ClH, SH_2--- SiH_4, PH_3---ClH, PH_3---FH, PH_3---SH_2, PH_3--- PH_3, PH_3---CH_4, PH_3---SiH_4, NH_3---ClH, NH_3---PH_3, NH_3---SiH_4, CH_4---ClH, CH_4---FH, CH_4---PH_3, CH_4---CH_4, CH_4--- SiH_4, SiH_4---ClH, SiH_4---FH, SiH_4---OH_2, SiH_4---SH_2, SiH_4---NH_3, SiH_4---PH_3, and SiH_4---CH_4. This list thus includes 11 of the Si models (~70% of the total of 15 Si models), 9 of the P models, 4 of the S models, and 3 of the Cl models. There is thus a clear trend for heavier and softer elements to not engage in well-defined intermolecular element-hydrogen interactions – and this is especially true for Si and P. In the case of Si, this expectedly involves the Si in SiH_4 as an acceptor (due to sterical constraints by the tetrahedral coordination geometry at Si), but also the protons in SiH_4. Also marked in Tables 1 and 2 are the cases where D is smaller than R – i.e. cases where the intermolecular distance would be closer to the sum of covalent radii than to the sum of van der Waals radii. These particularly strong interactions involve the pairs ClH---OH_2, ClH---NH_3, FH---FH, FH---OH_2, FH---NH_3, OH_2---ClH, OH_2---FH, and NH_3---FH –dominantly involving the two most electronegative elements of the set examined here – fluorine (5 out of 8 pairs on the list) and oxygen (4) , followed closely by their neighbors nitrogen and chlorine (3 instances each).

For the H---Cl the interaction energy is in most systems ~0.6 kcal/mol, with values ranging from 0.4 kcal/mol for the HCl dimer HCl to 2.5 kcal/mol for the HF/HCl pair. For the H---F interaction, the values range from 5.7 kcal/mol in the HF dimer to 0.6 kcal/mol in the pairs with CH_4 and PH_3. For H---O, the energies range from 9.4 kcal/mol in the H_2O/HF pair, to 1.4 kcal/mol in the HF/SiH_4 pair. For the H---S interaction, the values range from 4.4 kcal/mol for the H_2S/HF pair to 0.6 kcal/mol with PH_3. For the H---N interactions, energies range from 13.2 kcal/mol in the NH_3 pairs with HCl or HF, to 0.6 kcal/mol in the pairs with PH_3, CH_4 and SiH_4. For the H---P interaction, the

lowest energy is found in the PH_3/CH_4 pair with 0.2 kcal/mol, while the strongest interaction is in the PH_3/HF pair, with 4.4 kcal/mol. The H---C interaction is a weak one regardless of the system components, ranging from 0.5 kcal/mol in the methane dimer to 1.3 in the CH_4/HF pair. The H---Si interaction is also of weak intensity, ranging from 0.6 kcal/mol (in the SiH_4 pairs with HF or CH_4) to 2.5 kcal /mol in the water/SiH_4 pair.

Table 1. H---X intermolecular distances (D, Å), sums of van der Waals radii (vdW, Å), average between vdW and the sums of covalent radii (R, Å) and interaction energies (kcal/mol) for XH_n---YH_m systems with X = Cl, F, O, S. BP86 data are shown in grey. *Italics: D>vdW*; **bold: D<R**.

dimer	contact	R	vdW	D	ΔE	D	ΔE
ClH---ClH	H---Cl	2.15	2.95	*3.27*	0.41	4.8	0.15
ClH---FH	H---F	1.87	2.67	1.97	3.8	1.9	3.61
ClH---OH_2	H---O	1.91	2.72	**1.85**	7.28	1.75	7.83
ClH---SH_2	H---S	2.19	3.00	2.50	3.55	2.34	3.93
ClH---NH_3	H---N	1.93	2.75	**1.67**	11.71	1.62	13.25
ClH---PH_3	H---P	2.21	3.00	2.58	3.51	2.42	3.66
ClH---CH_4	H---C	2.00	2.90	2.52	1.11	2.63	0.20
ClH---SiH_4	H---Si	2.58	3.30	3.12	0.71	9.27	0.00
FH---ClH	H---Cl	2.15	2.95	2.45	2.51	2.45	1.88
FH---FH	H---F	1.87	2.67	**1.82**	5.65	1.81	5.02
FH---OH_2	H---O	1.91	2.72	**1.75**	9.41	1.74	8.79
FH---SH_2	H---S	2.19	3.00	2.40	4.39	2.35	4.39
FH---NH_3	H---N	1.93	2.75	**1.75**	13.18	1.73	13.18
FH---PH_3	H---P	2.21	3.00	2.49	4.39	2.43	3.77
FH---CH_4	H---C	2.00	2.90	2.38	1.26	2.49	0.63
FH---SiH4	H---Si	2.58	3.30	3.05	0.63	3.23	0.63
OH_2---ClH	H---O	1.91	2.72	**1.85**	7.53	1.75	7.53
OH_2---FH	H---O	1.91	2.72	**1.76**	9.41	2.01	2.51
OH_2---OH_2	H---O	1.91	2.72	1.95	6.28	1.94	5.02
OH_2---SH_2	H---S	2.19	3.00	2.61	3.14	2.60	2.51
OH_2---NH_3	H---N	1.93	2.75	1.98	7.53	1.94	6.90
OH_2---PH_3	H---P	2.21	3.00	2.71	2.51	2.73	1.88
OH_2---CH_4	H---C	2.00	2.90	2.56	0.63	2.90	0.00
OH_2---SiH_4	H---Si	2.58	3.30	*3.54*	2.51	4.73	0.00
SH_2---ClH	H---Cl	2.15	2.95	*3.06*	0.63	2.87	0.63
SH_2---FH	H---F	1.87	2.67	2.19	1.88	2.19	1.26
SH_2---OH_2	H---O	1.91	2.72	2.11	3.77	2.04	3.14
SH_2---SH_2	H---S	2.19	3.00	2.86	1.88	2.73	1.26
SH_2---NH_3	H---N	1.93	2.75	2.12	5.02	1.99	5.65
SH_2---PH_3	H---P	2.21	3.00	2.92	1.88	2.84	1.26
SH_2---CH_4	H---C	2.00	2.90	2.76	0.63	5.42	0.00
SH_2---SiH_4	H---Si	2.58	3.30	*3.66*	1.26	6.73	0.00

Table 2. H---X intermolecular distances (D, Å), sums of van der Waals radii (vdW, Å), average between vdW and the sums of covalent radii (R, Å) and interaction energies (kcal/mol) for XH_n---YH_m systems with X = P, N, C, Si. BP86 data are shown in grey. *Italics: D>vdW*; **bold: D<R**.

dimer	contact	R	vdW	D	ΔE	D	ΔE
PH_3---ClH	H---Cl	2.15	2.95	*3.21*	0.63	5.65	0.00
PH_3---FH	H---F	1.87	2.67	*2.77*	0.63	2.43	3.77
PH_3---OH_2	H---O	1.91	2.72	2.44	1.26	2.52	0.63
PH_3---SH_2	H---S	2.19	3.00	*3.21*	0.63	5.4	0.00
PH_3---NH_3	H---N	1.93	2.75	2.52	1.26	2.44	1.26
PH_3---PH_3	H---P	2.21	3.00	*3.61*	1.26	3.69	0.00
PH_3---CH_4	H---C	2.00	2.90	*3.23*	0.63	6.08	0.00
PH_3---SiH_4	H---P	2.21	3.00	*3.26*	1.26	8.05	0.00
NH_3---ClH	H---Cl	2.15	2.15	*3.10*	0.63	1.62	13.18
NH_3---FH	H---N	1.93	2.75	**1.75**	13.18	1.73	13.18
NH_3---OH_2	H---N	1.93	2.75	1.98	7.53	2.18	2.51
NH_3---SH_2	H---N	1.93	2.75	2.12	5.02	1.99	5.65
NH_3---NH_3	H---N	1.93	2.75	2.21	3.77	2.19	3.14
NH_3---PH_3	H---N	1.93	2.75	*3.04*	0.63	3.07	2.51
NH_3---CH_4	H---N	1.93	2.75	2.60	0.63	5.25	0.00
NH_3---SiH_4	H---Si	2.58	2.58	*3.35*	1.26	13.38	0.00
CH_4---ClH	H---Cl	2.15	2.95	*3.31*	0.63	5.85	0.00
CH_4---FH	H---F	1.87	2.67	*2.69*	0.63	3.90	0.00
CH_4---OH_2	H---O	1.91	2.72	2.46	0.63	2.74	0.00
CH_4---SH_2	-	-	-	-		5.88	0.63
CH_4---NH_3	H---N	1.93	2.75	2.57	0.63	2.66	0.63
CH_4---PH3	H---P	2.21	3.00	*3.64*	0.23	5.80	0.01
CH4---CH_4	H---C	2.00	2.90	*3.30*	0.49	5.68	0.38
CH_4---SiH_4	H---Si	2.58	3.30	3.23	0.63	7.30	0.00
SiH_4---ClH	H---Cl	2.15	2.95	*3.33*	0.21	6.27	0.00
SiH_4---FH	H---F	1.87	2.67	*2.91*	1.26	4.03	0.00
SiH_4---OH_2	H---O	1.91	2.72	*3.29*	0.00	4.08	0.00
SiH_4---SH_2	H---S	2.19	3.00	*3.06*	1.26	6.37	0.00
SiH_4---NH_3	H---N	1.93	2.75	*2.92*	3.14	11.51	0.00
SiH_4---PH_3	H---P	2.21	3.00	*3.18*	1.26	6.70	0.00
SiH_4---CH_4	H---C	2.00	2.90	*3.33*	0.63	6.65	0.00
SiH_4---SiH_4	H---Si	2.58	3.30	3.17	1.26	7.11	0.00

In the following, the results obtained with the BP86 functional will be briefly discussed, specifying that the assemblies in which the intermolecular distance is greater than 5 Å have been excluded from the discussion. The average distances (obtained by calculating the arithmetic mean of all interactions of the same type from different systems) for each type of interaction are: H---Cl 3.37 Å, H---F 2.64 Å, H---O 2.30 Å, H---S 2.505 Å, H---N 1.99 Å, H---P 2.80 Å,

H---C 2.67 Å, H---Si 3, 98 Å. Compared to the calculated average distances, the closest and most distant interactions are found at the following distances for each type of interaction: H---Cl 0.50 Å, respectively 1.43 Å, H---F 0.45 Å, respectively 1.39 Å, H---O 0.12 Å, respectively 1.78 Å, H---S 0.10 Å, respectively 0.23 Å, H---N 0 Å, respectively 0 .67 Å, H---P 0.07 Å and 0.89 Å respectively, H---C 0.04 Å and 0.23 Å respectively, H---Si 0.75 Å. Relative to R, the closest and most distant interactions are found at the following distances for each type of interaction: H---Cl 0.30 Å and 2.65 Å respectively, H---F 0.03 Å, respectively 2.03 Å, H---O 0.03 Å respectively 2.17 Å, H---S 0.15 Å respectively 0.54 Å, H---N 0.01 Å respectively 0 .73 Å, H---P 0.21 Å, respectively 1.48 Å, H---C 0.49 Å, respectively 0.9 Å, H---Si 0.65 Å, respectively 2.15 Å. The smallest distances identified for each type of interaction are: H---Cl 2.45 Å, H---F 1.81 Å, H---O 1.74 Å, H---S 2.34 Å, H---N 1.62 Å, H---P 2.42 Å, H---C 2.49 Å, H---Si 3.23 Å. The BP86 functional often fails to give ΔE of the order of kcal/mol, in many cases ΔE being approximated to 0 kcal/mol. Overall, we find that in general the BP86 functional leads to energy differences ΔE that are smaller than those obtained using the M06-2X functional. Regarding the distances between the atoms involved in the non-covalent interaction, there are significant differences between the results obtained with the two functionals, especially in the case of systems containing larger molecules. If one averages all the distances obtained with the two functionals, a value of 2.68 Å is obtained for the M06-2X functional and an average of 3.94 Å for the BP86 functional. In the case of energies, an average of 2.9 kcal/mol is obtained for the M06-2X functional, and 2.5 kcal/mol for the BP86 functional. Even if the difference between these averages does not seem large at first glance, upon closer analysis we find that in fact the higher values obtained compensate for those approximated by 0. As a general note, the very small values seen even with M06-2X should be interpreted with caution – especially when below 2 kcal/mol. While the trends are expected to be correctly reproduced, the exact values may still be in error and in principle even improved by more accurate post-HF approaches and/or further corrections (e.g., counterpoise, dispersion).

Figure 1 illustrates the correlations between the Mulliken partial atomic charges on the two units – which are an indication of the degree of polarity of the interaction - and the binding energies, at R^2~0.7. Better correlations are seen in the pairs with stronger overall interactions and with more linear X-H---Y geometries (e.g., 0.97 for ClH---YHm in Figure 2). These numbers illustrate the predominantly/majorly electrostatic nature of the non-covalent intermolecular interactions examined here, in line with considerations consistently made about hydrogen bonds in general, but not only.[5,6]

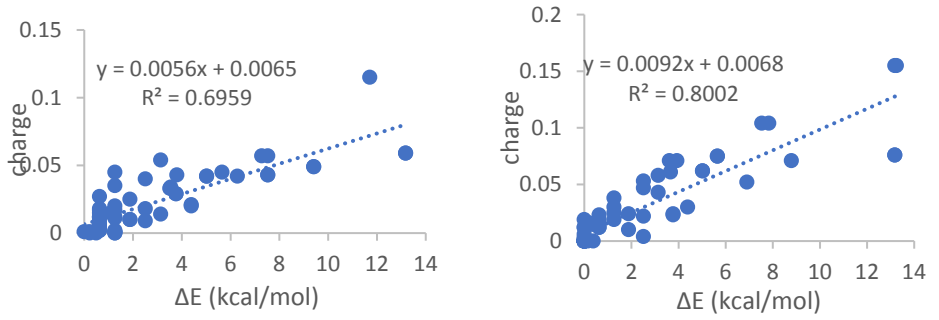

Figure 1. Correlation between the binding energies (ΔE) and Mulliken atomic charges, from M06-2X (left) and BP86 (right) calculations.

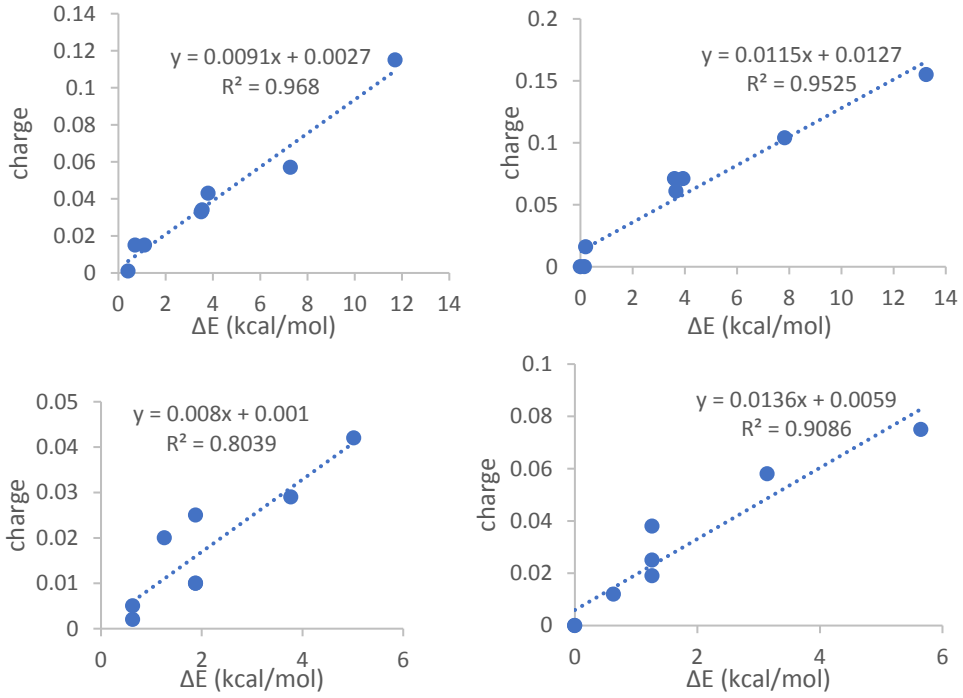

Figure 2. Correlations between the binding energies (ΔE) and Mulliken charges, from M06-2X (left) and BP86 (right) calculations for the ClH-YH_m (top) and OH_2---YH_m (bottom) sets of models.

The vibration frequencies for all models have been compared with the frequencies seen in the molecule whose hydrogen was involved in the interaction in the initial geometry. A large number of intermolecular vibrations may be noted; this is expected to impact the total energy of the system. Most of these frequencies occur in regions rarely explorable experimentally for large molecules of practical interest (i.e., below 400 cm^{-1} – although this is somewhat of a circular comment since such vibrations from the solvent/ medium will be those responsible for the experimental limitations). However, larger values are seen for the models where the proton donors in the XH_n---YH_m dimers are NH_3, FH or ClH (up to~1000 cm^{-1}), OH_2 (up to ~800 cm^{-1}), SH_2 and PH_3 (up to ~5-600 cm^{-1}). It is expected that such frequencies should be observable not only in such dimeric mixtures as analyzed here, but also in more complex environments, including ones where the element-hydrogen bonds examined here are in fact parts of more complex molecular structures (indeed, while most of the larger frequencies involve the strong acids HF and HCl which would be dissociated in water, several of them also only involve only water, hydrogen sulfide and ammonia – which may be taken as prototypes of hydroxyl, amino and sulfhydryl groups, respectively). Such intermolecular vibrations are inherently ignored in most rationalizations of vibrational spectra when (as usually is the case) monomolecular models are employed.

Also of practical interest, we may note that the inherent vibrations of the hydrogen-donating molecule shift upon interaction with the various partners by a various degrees: up to 10 cm^{-1} in CH_4 but with a few exceptions of up to 200 cm^{-1} at high frequencies, similarly in SiH_4 (but with exceptions only going up to ~20 cm^{-1}), NH_3 (one exception of ~70 cm^{-1} at ~1100 cm^{-1}), and PH_3 (exceptions of up to ~40 cm^{-1}). For OH_2, distinct effects are seen, of 40 and 130 cm^{-1} for two of the total of three bands ion the spectrum; SH_2 behaves somewhat similarly, although with smaller effects than seen in OH_2. For FH and ClH, the effects are even larger (600 and 900 cm^{-1}, respectively). Overall, the strength of the intermolecular effects on the vibrational spectrum is thus (expectedly) seen to increase with the strength of the intermolecular interaction and to be more efficient in systems with well-aligned $H_{n-1}X$-H---YH_m units (especially those involving diatomics, and more efficiently for lower values of n and m).

The importance of solvation is well recognized in predicting molecular structures and properties, including spectra.[28–30] However, in most cases implicit solvation models are employed, or, more rarely, relatively small explicit models. The results shown here may suggest that explicit solvation may be essential for describing spectroscopic properties in cases where stronger and directionally well-defined supramolecular interactions occur.

On a methodological note, when comparing the M06-2X functional to BP86, a decrease in vibration frequency values by 3-5% is observed. The largest discrepancy occurs in the case of the SiH4 molecule, 6.5%, and the smallest in the case of the water molecule, 0.8%.

Further on methodological aspects, Tables 3 and 4 illustrate representative data from energy decomposition analyses on two extreme cases from our set of dimers – CH_4---CH_4 and HF---HF from M06-2X calculations (with similar data available for BP86 calculations). The electrostatic component of the interaction energy in Tables 3 and 4 is in fact seen to be almost identical between the methane dimer vs. the HF dimer – despite the fact that the total interaction energy is stronger by ~5 kcal/mol in the HF case (and essentially zero in the methane case). The above-discussed data on Mulliken charges does convincingly show correlations between the interaction energies and the magnitude of charge separation. Interestingly, Tables 3 and 4 suggest this to be mere correlation and not causation. Instead, a notable part of the ~5 kcal/mol interaction energy within the HF dimer appears to originate from the difference between the sterical and the quantum effects. These two terms in turn are derived from quantities enumerated in the upper rows of Tables 3 and 4.

Table 3. Extended Transition State - Natural Orbitals for Chemical Valence (ETS-NOCV) analysis and Shubin Liu's energy decomposition analysis (EDA-SBL) for the CH_4---CH_4 structure optimized with M06-2X.

Type of Energy	**Energy (Hartree)**			**Energy (kcal/mol)**
ETS-NOCV energy decomposition terms	Full structure CH_4—CH_4	Fragment 1 CH_4	Fragment 2 CH_4	ΔE
Electronic kinetic energy (ET)	80.639	40.321	40.317	-0.137
Weizsacker kinetic energy (TW)	65.539	32.780	32.780	-13.368
Interelectronic Coulomb repulsion energy (EJ)	77.694	32.852	32.842	7530.332
Internuclear Coulomb repulsion energy (ENuc)	39.045	13.526	13.516	7531.834
Nuclear-electronic Coulomb attraction energy (EV)	-264.602	-120.311	-120.288	-15061.920
Energy without electronic correlation (ET+EV+EJ+ENuc)	-67.224	-33.612	-33.613	0.109
Exchange correlation energy (Ex)	-13.065	-6.533	-6.532	0.315
Coulomb correlation energy (Ec)	-0.776	-0.388	-0.388	-0.312
Pauli kinetic energy (ET-TW)	15.100	7.542	7.537	13.230
EDA-SBL energy decomposition terms				
E_steric:	65.539	32.780	32.780	-13.368
E_electrostatic:	-147.863	-73.933	-73.930	0.246
E_quantum:	1.259	0.620	0.617	13.233
E_total:	-81.065	-40.533	-40.533	0.111

Some of the latter are dependent on the total number of particles in the system, but one may note that the correlation effects are essentially zero on the methane dimer, but amount to ~70% of the total interaction energy in the HF dimer. The intrinsic asymmetry of the monomeric units (HF vs. methane) may in principle be a common cause for both the subsequent charge separation and correlation. However, confirmation and full exploration of such hypotheses would require a systematic analysis of the set of dimers, as opposed to only the two extremes – which is within the scope of a subsequent report.

Table 4. Extended Transition State - Natural Orbitals for Chemical Valence (ETS-NOCV) analysis and Shubin Liu's energy decomposition analysis (EDA-SBL) for the FH---FH structure optimized with M06-2X.

Type of Energy	**Energy (Hartree)**			**Energy (kcal/mol)**
ETS-NOCV energy decomposition terms	Full structure FH--FH	Fragment 1 FH	Fragment 2 FH	ΔE
Electronic kinetic energy (ET)	200.834	100.419	100.419	-2.172
Weizsacker kinetic energy (TW)	146.106	73.124	73.124	-89.795
Interelectronic Coulomb repulsion energy (EJ)	131.979	56.050	56.050	12473.902
Internuclear Coulomb repulsion energy (ENuc)	30.883	5.412	5.412	12587.314
Nuclear-electronic Coulomb attraction energy (EV)	-542.861	-251.462	-251.462	-25060.665
Energy without electronic correlation (ET+EV+EJ+ENuc)	-179.165	-89.581	-89.581	-1.621
Exchange correlation energy (Ex)	-20.842	-10.420	-10.420	-1.524
Coulomb correlation energy (Ec)	-0.935	-0.466	-0.466	-1.912
Pauli kinetic energy (ET-TW)	54.729	27.294	27.294	87.623
EDA-SBL energy decomposition terms				
E_steric:	146.106	73.124	73.124	-89.795
E_electrostatic:	-379.999	-190.000	-190.000	0.551
E_quantum:	32.951	16.409	16.409	84.187
E_total:	-200.942	-100.467	-100.467	-5.057

EXPERIMENTAL SECTION

Dimeric models XH_n---YH_m, where n,m=1-4 and X and Y are C, Si, N, P, O, S, F and Cl, respectively (i.e., involving HF, HCl, H_2O, H_2S, NH_3, PH_3, CH_4 and SiH_4), were built using the Spartan[31] graphical interface so that there would be a linear X---H-Y unit, with the X---H distance slightly below the sum of van der Waals radii. Geometries were optimized using the M06-2X and

BP86 functionals and the 6-311G(d,p) basis set within the Gaussian software package.[32] Vibrational spectra were verified so that no negative frequencies would be present (i.e., the structures were true energy minima). Solvation was not included, as most of the systems examined here would not be viable in usual solvents (either because of dissociation, or because of solvation). Relative energies (ΔE) listed in Tables 1 and 2 represent the difference between the energy of the energy of the XH_n---YH_m pair and the isolated XH_n and YH_m systems calculated separately; positive values imply an attractive interaction.

For the energy decomposition analysis Multiwfn[33] was used. With the Extended Transition State - Natural Orbitals for Chemical Valence (ETS-NOCV) analysis[34–36] method, the energy decomposition terms were calculated, where the structures was separated in two main fragments. The steric, electrostatic, quantum and total energies were calculated with Shubin Liu's energy decomposition (EDA-SBL)[37] method.

CONCLUSIONS

Reported here is a systematic computational analysis of such interactions within XH_n---YH_m dimers, where X and Y are C, Si, N, P, O, S, F and Cl, respectively. The interaction energies are found to be correlated with charge separation to a degree of 80%, suggesting that these noncovalent interactions can be reasonably explained/predicted by their electrostatic component – though energy decomposition analyses exploring the phenomenon in more detail appear to indicate a role for correlation effects more so than electrostatics. The rarely discussed intermolecular vibrations are also analyzed and noted to sometimes intercede in the typical observation windows for molecular spectroscopy. Moreover, in some cases notable effects of the non-covalent interactions are noted upon internal vibrations of the partners.

ACKNOWLEDGMENTS

Drs. Daniela Cioloboc and Adrian M.V Brânzanic (UBB) are thanked for helpful discussions and technical support.

Supporting Information available

Tables containing vibrational frequencies, Figures illustrating geometries – available upon request from the authors.

REFERENCES

1. Zhao, Y.; Truhlar, D. G. A *J. Chem. Phys.* **2006**, No. 125, 194101–194118.
2. Zhao, Y.; Truhlar, D. G. *Theor. Chem. Acc.* **2008**, *120*, 215–241.
3. Grimme, S. *J. Comput. Chem.* **2006**, *27*, 1787–1799. https://doi.org/10.1002/jcc.
4. Radu, L. BSc Diploma Paper: Studiul Interacțiunilor Necovalente. Studii Experimentale Și Teoretice, Babes-Bolyai University, 2014.
5. Silaghi-Dumitrescu, L.; Attia, A. A. A.; Silaghi-Dumitrescu, R.; Blake, A. J.; Sowerby, D. B. *Inorg. Chim. Acta* **2018**, *475*, 120–126. https://doi.org/10.1016/j.ica.2017.08.052.
6. Silaghi-Dumitrescu, R.; Lupan, A. *Cent. Eur. J. Chem.* **2013**, *11* (3), 457–463.
7. Irsai, I.; Majdik, C.; Lupan, A.; Silaghi-Dumitrescu, R. *J. Math. Chem.* **2012**, *50* (4), 703–733.
8. Carrascoza, F.; Zaric, S.; Silaghi-Dumitrescu, R. *J. Mol. Graph. Model.* **2014**, *50*, 125–133.
9. Irsai, I.; Pesek, S. Z.; Silaghi-Dumitrescu, R. *Studia UBB Chemia.* **2022**, *67* (4), 47–72.
10. Irsai, I.; Lupan, A.; Majdik, C.; Silaghi-Dumitrescu, R. *Studia UBB Chemia.* **2017**, *62* (4), 495–513.
11. Silaghi-Dumitrescu, R. *Studia UBB Chemia.* **2010**, *60(1),* 31–36.
12. Lupan, A.; Kun, A.-Z. Z.; Carrascoza, F.; Silaghi-Dumitrescu, R. Performance *J. Mol. Model.* **2013**, *19* (1), 193–203.
13. Carrascoza Mayen, J. F.; Lupan, A.; Cosar, C.; Kun, A.-Z.; Silaghi-Dumitrescu, R. *Biophys. Chem.* **2015**, *197*, 10–17.
14. Pesek, S.; Lehene, M.; Brânzanic, A. M. V.; Silaghi-Dumitrescu, R. *Molecules* **2022**, *27* (24), 8974.
15. Hobza, P.; Řezáč, J. *Chem. Rev.* **2016**, *116* (9), 4911–4912.
16. Sexton, T. M.; Howard, J. C.; Tschumper, G. S. *J. Phys. Chem. A* **2018**, *122* (21), 4902–4908.
17. Leverentz, H. R.; Truhlar, D. G. *J Phys Chem A* **2008**, *112* (26), 6009–6016.
18. Zhao, Y.; Truhlar, D. G. *J. Phys. Chem. A* **2005**, *109* (25), 5656–5667.
19. Silaghi-Dumitrescu, R.; Silaghi-Dumitrescu, I. *J. Inorg. Biochem.* **2006**, *100* (1), 161–166.
20. Attia, A. A. A.; Silaghi-Dumitrescu, R. A *J. Mol. Graph. Model.* **2016**, *69*, 103–110.
21. Xie, Y. M.; Schaefer, H. F.; Silaghi-Dumitrescu, R.; Peng, B.; Li, Q. S.; Stearns, J. A.; Rizzo, T. R. *Chem. Eur. J.* **2012**, *18* (41), 12941–12944.
22. Attia, A. A. A.; Lupan, A.; Silaghi-Dumitrescu, R. *RSC Adv.* **2013**, *3* (48), 26194–26204.
23. Brânzanic, A. M. V.; Ryde, U.; Silaghi-Dumitrescu, R. I *J. Inorg. Biochem.* **2020**, *203*, 110928.
24. Silaghi-Dumitrescu, R. A *Studia UBB Chemia,* **2007**, *52* (2), 127–139.
25. Silaghi-Dumitrescu, R.; Silaghi-Dumitrescu, I. *Rev. Roum. Chim.* **2004**, *49*, 257–268.

26. Surducan, M.; Makarov, S. V.; Silaghi-Dumitrescu, R. *Eur. J. Inorg. Chem.* **2014**, *34* (34), 5827–5837..
27. Attia, A. A. A.; Cioloboc, D.; Lupan, A.; Silaghi-Dumitrescu, R. *J. Inorg. Biochem.* **2016**, *165*, 49–53.
28. Tomasi, J.; Mennucci, B.; Cammi, R. *Chem. Rev.* **2005**, *105* (8), 2999–3093.
29. Barone, V.; Cossi, M. *J. Phys. Chem. A* **1998**, *102* (97), 1995–2001.
30. Klamt, A.; Jonas, V.; Bürger, T.; Lohrenz, J. C. W. *J. Phys. Chem. A* **1998**, *102* (26), 5074–5085.
31. SPARTAN '18 for Windows, Wavefunction Inc., 18401 Von Karman Avenue, Suite 370 Irvine, CA 92612. 2018.
32. Frisch, M. J.; Trucks, G. W.; Schlegel, H. B.; Scuseria, G. E.; Robb, M. A.; Cheeseman, J. R.; Scalmani, G.; Barone, V.; Petersson, G. A.; Nakatsuji, H.; Li, X.; Caricato, M.; Marenich, A.; Bloino, J.; Janesko, B. G.; Gomperts, R.; Mennucci, B.; Hratchian, H. P.; Ortiz, J. V.; Izmaylov, A. F.; Sonnenberg, J. L.; Williams-Young, D.; Ding, F.; Lipparini, F.; Egidi, F.; Goings, J.; Peng, B.; Petrone, A.; Henderson, T.; Ranasinghe, D.; Zakrzewski, V. G.; Gao, J.; Rega, N.; Zheng, G.; Liang, W.; Hada, M.; Ehara, M.; Toyota, K.; Fukuda, R.; Hasegawa, J.; Ishida, M.; Nakajima, T.; Honda, Y.; Kitao, O.; Nakai, H.; Vreven, T.; Throssell, K.; MontgomeryJr., J. A.; Peralta, J. E.; Ogliaro, F.; Bearpark, M.; Heyd, J. J.; Brothers, E.; Kudin, K. N.; Staroverov, V. N.; Keith, T.; Kobayashi, R.; Normand, J.; Raghavachari, K.; Rendell, A.; Burant, J. C.; Iyengar, S. S.; Tomasi, J.; Cossi, M.; Millam, J. M.; Klene, M.; Adamo, C.; Cammi, R.; Ochterski, J. W.; Martin, R. L.; Morokuma, K.; Farkas, O.; Foresman, J. B.; Fox, D. J. Gaussian 09, Revision E.01. *Gaussian 09, Revision E.01, Gaussian, Inc., Wallingford CT, 2016*. Gaussian, Inc.: Wallingford CT, 2016.
33. Lu, T.; Chen, F. *J. Comput. Chem.* **2012**, *33* (5), 580–592.
34. Mitoraj, M. P.; Michalak, A.; Ziegler, T. *J. Chem. Theory Comput.* **2009**, *5* (4), 962–975.
35. Michalak, A.; Mitoraj, M.; Ziegler, T. *J. Phys. Chem. A* **2008**, *112* (9), 1933–1939.
36. Ziegler, T.; Rauk, A. *Theor. Chim. Acta* **1977**, *46* (1), 1–10..
37. Cao, X.; Liu, S.; Rong, C.; Lu, T.; Liu, S. *Chem. Phys. Lett.* **2017**, *687*, 131–137.